RSC Advances

COMMUNICATION

View Article Online
View Journal | View Issue

Cite this: *RSC Adv.*, 2016, **6**, 9175

Received 7th December 2015
Accepted 14th January 2016

DOI: 10.1039/c5ra26053a

www.rsc.org/advances

Filling nanoporous polymer thin films: an easy route toward the full control of the 3D nanostructure†

G. Li-Destri,*[a] A. Tummino,[ab] A. A. Malfatti Gasperini,[ac] L. Parellada Monreal,[a] G. M. L. Messina,[b] V. Spampinato,[d] G. Ceccone[d] and O. Konovalov*[a]

A novel approach enabling the full control of the 3D nanostructure of polymer thin films is presented. An ordered nanoporous polymer film is obtained using a nanoparticle monolayer as template. The pores are then filled with a second organic component *via* spin coating which, by modulating the deposition parameters, enables the control of the filling degree with nanometric precision.

Nanostructured polymer thin and ultrathin films have recently emerged as model systems to study the soft matter behavior under nano-confinement[1–3] as well as promising active materials in a number of applications such as electronics,[4] photovoltaics,[5] biosensing[6,7] and biomaterials.[8] In most of these cases it is of paramount importance to control the film nanostructure, as well as the polymer conformation, to clearly define the confinement condition of the polymer[9] or to optimize the device properties.[10] The most common approaches to attain this goal are exploiting the self-assembly properties of the polymer itself,[11,12] tuning the interactions with the substrate in order to tune polymeric orientation[13–16] or applying the so called top-down techniques, consisting of different approaches based on lithography,[17] use of both organic[18–25] and inorganic templates,[26–28] interaction of polymer with light[29] and application of external forces.[30] However, it is generally possible to control the film nanostructure only toward one direction with respect to the surface, that is in parallel or perpendicularly, and only in special cases, mainly involving block copolymers, a full 3D control is attainable.[31] For many technological applications this lack of three-dimensional control of the nanostructure is one of the main drawbacks limiting the full exploitation of polymer films.

On this view porous polymer films[32] would be promising candidates for controlling not only the horizontal but also the vertical nanostructure by filling them, in a tailored manner, with a second component. However, the established methods to obtain nanoscopic polymer pores are generally based on the self-assembly of block copolymers or polymer blends,[33,34] thus they do not enable a precise control of the chemical composition of the film. It will be shown here that it is possible to obtain narrowly dispersed nanoporous homopolymer ultrathin films *via* the soft colloidal lithography[35,36] and then to control their degree of filling. The method, schematized in Fig. 1A, consists of both the formation of a monolayer of hexagonally close packed silica nanoparticles and the filling of the monolayer interstices with a polymer film. Finally, by etching the silica nanoparticles with HF, polymer films with hexagonally close packed pores are obtained. These pores can be filled with a second organic component by spin coating and the degree of filling can be controlled by varying the solution concentration and/or the spin rate. Our approach has been applied to the poly(3-hexylthiophene) (P3HT) and [6,6]-phenyl-C61-butyric acid methyl ester (PCBM) blend, in view of its extensive use as active layer in organic photovoltaics where a careful control of both in-plane and out-of-plane nanostructure is required for maximizing the efficiency.[10,37,38]

Fig. 1B and C show the atomic force microscopy (AFM) topographical images of the 147 nm nominal diameter silica nanoparticles monolayer and of the polymer film after the silica etching. As it is evident, the porous structure keeps the same hexagonal array of the nanoparticles.

In order to verify that the HF etching does not affect the polymer chemical composition, an X-ray photoelectron spectroscopy (XPS) analysis, which allows to characterize both the elemental composition and the chemical bonds of polymer

[a]*ESRF-The European Synchrotron, 71, Avenue des Martyrs, Grenoble, France . E-mail: giolides@unict.it; konovalo@esrf.fr*

[b]*Laboratory for Molecular Surfaces and Nanotechnology (LAMSUN), Department of Chemistry, University of Catania and CSGI, V.le A Doria 6, 95125 Catania, Italy*

[c]*Brazilian Synchrotron Light Laboratory, CNPEM, Caixa Postal 6192, CEP 13.083-970, Campinas, São Paulo, Brazil*

[d]*European Commission, Joint Research Centre, Institute for Health and Consumer Protection, TP 125, Via E. Fermi 2749, 21027, Ispra, VA, Italy*

† Electronic supplementary information (ESI) available: Materials and experimental methods, full 2D GISAXS pattern of the silica nanoparticles monolayer and of the porous pure P3HT film, 25 μm^2 AFM height image of the nanoparticles monolayer, GISAXS cuts at Q_z 0.28 $Å^{-1}$ of the porous P3HT films with different degrees of PCBM filling. See DOI: 10.1039/c5ra26053a

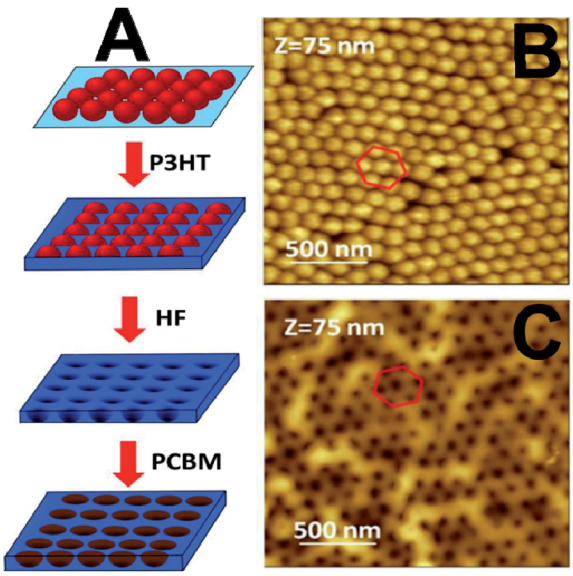

Fig. 1 Schematic representation of the nanoparticles-template method to obtain nanoporous polymer film (A). AFM height image of the nanoparticles layer (B) and of the nanoporous P3HT film upon the nanoparticles etching (C). The hexagonal packing of the nanoparticles, kept even after their removal, is highlighted in red.

thin films,[39,40] was performed on the porous P3HT film. These results were then compared to the ones of a flat HF-untreated P3HT film (Fig. 2). Both wide and elemental high resolution scans do not show any significant change between flat and porous P3HT films. In particular, the wide scan of the HF-treated sample does not show any signal coming from silicon or oxygen, confirming that the etching quantitatively removes the silica particles. Moreover, the carbon and sulphur high resolution scans are virtually identical for both samples, ensuring that the HF treatment does not alter the P3HT chemical composition.

Once obtained the porous P3HT film, it is possible to fill the pores with PCBM provided that the PCBM solution does not dissolve the polymer film. However, this issue can be easily solved by dissolving the PCBM in dichloromethane, which does not dissolve P3HT.[41] In order to ensure a homogeneous coverage and to control the degree of filling, PCBM was deposited *via* spin coating, enabling the control of the thickness of the deposited layer by tuning the spinning speed and the concentration of the spread solution. In Fig. 3 the AFM topographical images of the P3HT pores filled with PCBM at different concentrations and at two different spinning speeds are reported. It is clear, especially for low PCBM concentrations, that the spin coating process does not alter the hexagonal arrangements of the pores. Moreover, at a given spinning speed, the pores depth gradually decreases with increasing the PCBM concentration and only at 4.5 mg ml^{-1} the pores are not visible anymore. This trend is highlighted in Fig. 3I, where the depth of the pores as a function of the PCBM concentration is plotted, showing also that the spinning speed itself can be used to tune the amount of PCBM deposited at nanometric level. These results clearly show that, during the spin coating process, PCBM molecules are selectively deposited inside the pores and that it is possible to control the degree of filling, and therefore controlling the vertical nanostructure, by modulating the experimental parameters.

In order to extract quantitative structural information from the whole film thickness, grazing incidence X-ray small angle scattering (GISAXS) analysis was performed. GISAXS is a well established method to characterize the bulk nanostructure of ultrathin films[42] providing information on the size and shape of the nanostructured objects[43] as well as on their mutual assembly,[44] thus being perfectly complementary to pure surface techniques like AFM.

In Fig. 4A the experimental and simulated 2D GISAXS patterns of the silica particles monolayer are reported. The experimental pattern can be effectively simulated by considering a hexagonal array of nanoparticles having an average diameter of

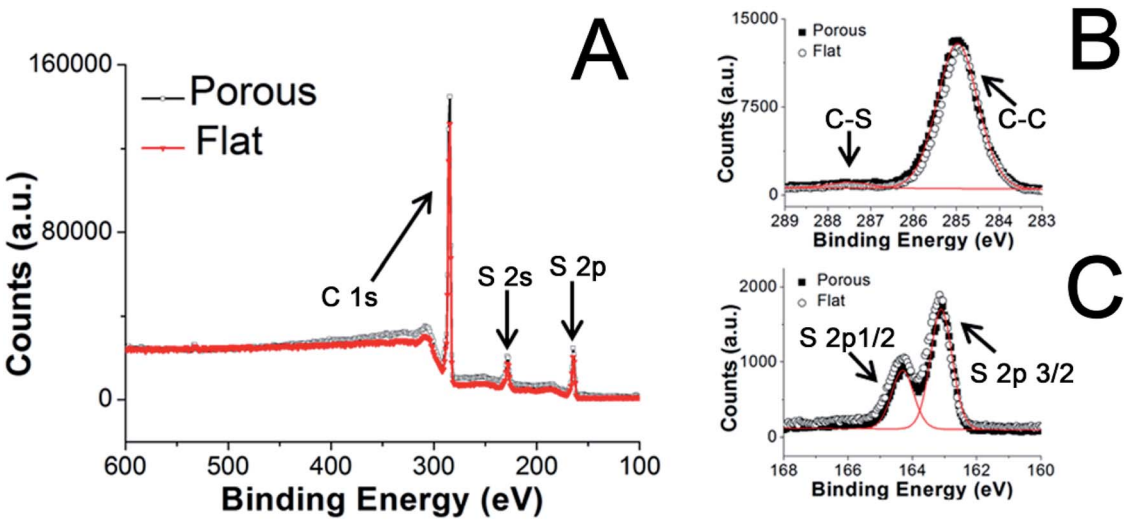

Fig. 2 XPS wide scan (A), high resolution C 1s (B) and S 2p (C) scans of the nanoporous and flat P3HT films. The continuous red lines in the high resolution scans show the individual component of the peaks.

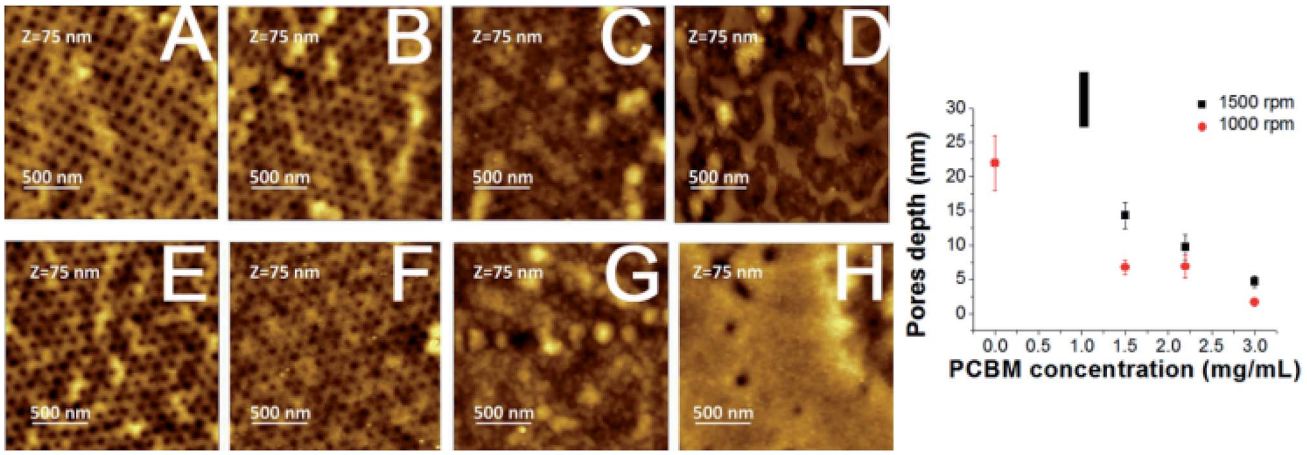

Fig. 3 AFM height images of the nanoporous P3HT film filled at 1500 rpm with PCBM solutions of 1.5 (A), 2.2 (B), 3.0 (C) and 4.5 (D) mg ml^{-1}. AFM height images of the nanoporous P3HT film filled at 1000 rpm with PCBM solutions of 1.5 (E), 2.2 (F), 3.0 (G) and 4.5 (H) mg ml^{-1}. Depth of the nanopores measured from the AFM images as a function of the PCBM concentration for both 1500 and 1000 rpm spinning speeds (I).

147 ± 6 nm. This low polydispersity gives rise to the numerous form factor hemi-circular rings around the reflected beam. The hexagonal arrangement leads instead to the formation of many the structure factor rods, whose length (see ESI Fig. S1†) is diagnostic of the presence of a 2D-ordered layer.[45]

It is finally worth to observe that the presence of higher orders structure factor rods are due to the large size of the 2D crystalline domains (around 10 μm^2), demonstrating the effectiveness of spin-coating as fast and easy method to obtain large 2D crystalline colloidal monolayer.

Upon etching the silica particles, the GISAXS pattern drastically changes (Fig. 4B) and no form factor signal from residual silica is observed, thus confirming the quantitative removal of the silica by HF. The weak contrast between pores and the polymer, as well as the increased uncorrelated irregularities of the pores shape, cause the extinction of the pores form factor

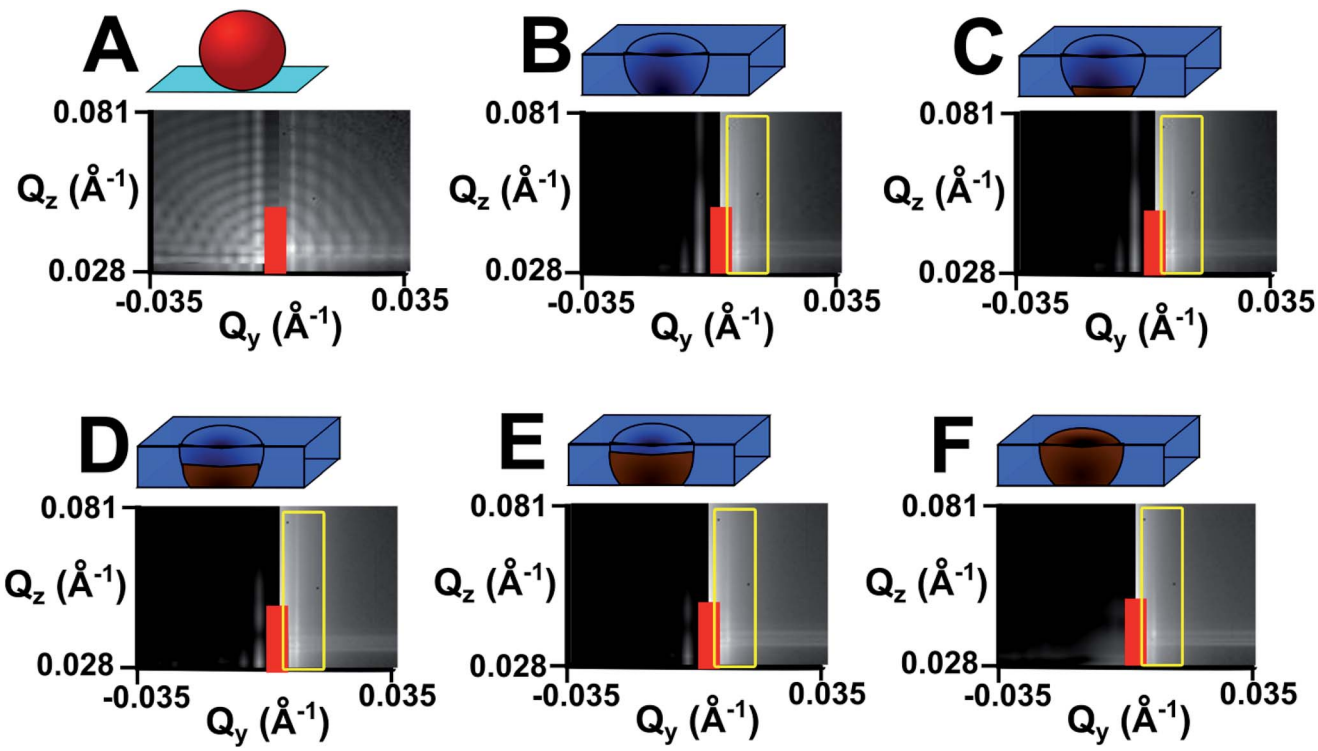

Fig. 4 Simulated (left) and experimental (right) GISAXS patterns of the nanoparticles monolayer (A), of the P3HT nanopores (B) and of the nanopores filled at 1500 rpm from PCBM solutions of concentration 1.5 (C), 2.2 (D), 3.0 (E) and 4.5 (F) mg ml^{-1}. Above each GISAXS pattern the pictorial representation of the form factor employed for the simulation is reported. The red rectangle between the experimental and simulated patterns represents the beamstop. The experimental structure factor rods are highlighted by the yellow box to facilitate the vision.

Table 1 Diameter and depth of the P3HT pores and the PCBM filling cores obtained from the GISAXS simulations

	P3HT pores	PCBM 1.5 mg ml^{-1} cores	PCBM 2.2 mg ml^{-1} cores	PCBM 3 mg ml^{-1} cores	PCBM 4.5 mg ml^{-1} cores
Diameter (nm)	40 ± 6	20 ± 6	24 ± 6	32 ± 9	40 ± 12
Depth (nm)	25 ± 1.5	7 ± 1.8	10 ± 2	20 ± 6	25 ± 6

manifestation on the GISAXS image. On the other hand, the structure factor rods are kept, because the pores maintain the hexagonal packing. Since the incoming X-ray beam samples the whole film thickness, a careful analysis of the GISAXS pattern allows determining the position of the pores across the film thickness itself and, more importantly, whether the bottom of the pore is covered by the polymer or not. The best simulation of the pores pattern is obtained by simulating truncated spheroidal air nanoparticles, having a diameter of 40 nm and a height of 25 nm, embedded in a 25 nm P3HT thin film. This means that the bottom of the pore is in direct contact with the native silicon oxide and explains why the PCBM selectively goes inside the pores. Indeed, since the silicon oxide surface free energy is much higher than the P3HT one,[46] the PCBM covers the residual exposed part of the substrate in order to minimize the overall surface free energy. The structural simulation also shows that the size distribution of the pores increases with respect to the silica particles (see Table 1), this is due to the inhomogeneous polymer coverage on the particle layer. This lack of homogeneity is mainly caused by the boundaries between nanoparticles ordered domains (see ESI Fig. S2†), where thicker P3HT layers are deposited. Finally, in Fig. 4C–F the GISAXS patterns of the P3HT pores filled at 1500 rpm with different PCBM concentrations are reported. It is evident that, by increasing the PCBM concentration, the scattering signal decreases and the rods become fainter. This effect is highlighted in ESI Fig. S3,† where the horizontal cuts of the pattern at Q_z 0.028 Å^{-1} are reported: the pure porous P3HT film shows three structure factor rods while, by increasing the PCBM concentration, the signal becomes progressively weaker and, at PCBM 4.5 mg ml^{-1}, only a very weak first order is observed. The main cause of this effect is the loss of electron density contrast when filling the organic P3HT pores with another organic component. Moreover, the increased polydispersity given by the pores filling also contributes to the signal weakening (see Table 1). An excellent agreement between GISAXS experimental and simulated patterns was obtained by considering truncated spheroidal core–shell particles, having a PCBM core and an air shell, embedded in the polymer matrix. The employed shell structural parameters were identical to the empty pore ones and were kept constant. The optimal core position was found to be on the bottom of the shell, thus confirming that PCBM effectively and uniformly fills the pores. Furthermore, its sizes were found to gradually increase with increasing the PCBM concentration (see Table 1), as a result of the gradual filling of the pores. The results of these simulations do not show, upon the spreading of the PCBM component, any significant increase of the thickness of the porous matrix, confirming the selective filling of the pores by PCBM.

Conclusions

We have reported a simple patterning methodology allowing to fully control the 3D nanostructures of polymer thin films. The method is based on the deposition of a nanoparticle monolayer that is used as a template to obtain nanoporous polymer films. The so-obtained pores can be then filled by a second component *via* spin coating and the degree of filling can be easily modulated by tuning the spinning speed and the concentration of the spread solution. This allows controlling with nanometre precision not only the in-plane nanostructure but also the out-of-plane one, and in turn the film chemical composition. We believe that our approach can be used to obtain fully controlled nanostructured polymer films enabling new experiments involving nano-confined soft matter. Moreover, the proper choice of the porous polymer and of the filling material will enable the preparation of a number of different 3D nanostructured polymeric and hybrid devices with great potential in many applications including membranes, electronics, photovoltaics, optical coatings, catalysis and sensing, among many other examples.

Acknowledgements

GL acknowledges the Surface Science Laboratory of the ESRF for AFM allocation and experimental support. AMG acknowledges Fapesp (processes 2013/13149-2 and 2011/19952-6) for financial support.

References

1 R. D. Priestley, C. J. Ellison, L. J. Broadbelt and J. M. Torkelson, *Science*, 2005, **309**, 456.
2 H. Atarashi, H. Morita, D. Yamazaki, M. Hino, T. Nagamura and K. Tanaka, *J. Phys. Chem. Lett.*, 2010, **1**, 881.
3 G. Li Destri, F. Miano and G. Marletta, *Langmuir*, 2014, **30**, 3345.
4 S. K. Gupta, P. Jha, A. Singh, M. M. Chehimi and D. K. Aswal, *J. Mater. Chem. C*, 2015, **3**, 8468.
5 Y. Yang, K. Mielczarek, M. Aryal, A. Zakhidov and W. Hu, *Nanoscale*, 2014, **6**, 7576.
6 K. Sandvold Beckwith, S. P. Cooil, J. W. Wells and P. Sikorski, *Nanoscale*, 2015, **7**, 8438; L. Xia, Z. X. Wei and M. X. Wan, *J. Colloid Interface Sci.*, 2010, **341**, 1.
7 G. Barbarella and F. Di Maria, *Acc. Chem. Res.*, 2015, **48**, 2230.
8 F. Brétagnol, A. Valsesia, G. Ceccone, P. Colpo, D. Gilliland, L. Ceriotti, M. Hasiwa and F. Rossi, *Plasma Processes Polym.*, 2006, **3**, 443.

9 Y. Y. Kim, B. Ahn, S. Sa, M. Jeon, S. V. Roth, S. Y. Kim and M. Ree, *Macromolecules*, 2013, **46**, 8235.
10 N. E. Jackson, B. M. Savoie, T. J. Marks, L. X. Chen and M. A. Ratner, *J. Phys. Chem. Lett.*, 2015, **6**, 77.
11 A. C. Shi and B. Li, *Soft Matter*, 2013, **9**, 1398.
12 I. P. Campbell, G. J. Lau, J. L. Feaver and M. P. Stoykovich, *Macromolecules*, 2012, **45**, 1587.
13 R. J. Kline, M. D. McGehee and M. F. Toney, *Nat. Mater.*, 2006, **5**, 222.
14 G. Li Destri, T. F. Keller, M. Catellani, F. Punzo, K. D. Jandt and G. Marletta, *Langmuir*, 2012, **28**, 5257.
15 R. Schulze, M. M. L. Arras, G. Li Destri, M. Gottschaldt, J. Bossert, U. S. Schubert, G. Marletta, K. D. Jandt and T. F. Keller, *Macromolecules*, 2012, **45**, 4740.
16 C. K. Shelton and T. H. Epps, *Macromolecules*, 2015, **48**, 4572.
17 C. F. Shih, K. T. Hung, J. W. Wu, C. Y. Hsiao and W. M. Li, *Appl. Phys. Lett.*, 2009, **94**, 143505.
18 A. Laiho, R. H. A. Ras, S. Valkama, J. Ruokolainen, R. Österbacka and O. Ikkala, *Macromolecules*, 2006, **39**, 7648.
19 I. Botiz, A. B. F. Martinson and S. B. Darling, *Langmuir*, 2010, **26**, 8756.
20 S. Y. Choi, J. U. Lee, J. W. Lee, S. Lee, Y. J. Song, W. H. Jo and S. H. Kim, *Macromolecules*, 2011, **44**, 1771.
21 A. Takahashi, Y. Rho, T. Higashihara, B. Ahn, M. Ree and M. Ueda, *Macromolecules*, 2010, **43**, 4843.
22 E. J. W. Crossland, M. Kamperman, M. Nedelcu, C. Ducati, U. Wiesner, D. M. Smilgies, G. E. S. Toombes, M. A. Hillmyer, S. Ludwigs, U. Steiner and H. J. Snaith, *Nano Lett.*, 2009, **9**, 2807.
23 I. Botiz and S. B. Darling, *Macromolecules*, 2009, **42**, 8211.
24 P. D. Topham, A. J. Parnell and R. C. Hiorns, *J. Polym. Sci., Part B: Polym. Phys.*, 2011, **49**, 1131.
25 S. B. Darling, *Prog. Polym. Sci.*, 2007, **32**, 1152.
26 H. S. Wang, S. Y. Chen, M. H. Su, Y. L. Wang and K. H. Wei, *Nanotechnology*, 2010, **21**, 145203.
27 K. M. Coakley and M. D. McGehee, *Appl. Phys. Lett.*, 2003, **83**, 3380.
28 W. C. Yen, Y. H. Lee, J. F. Lin, C. A. Dai, U. S. Jeng and W. F. Su, *Langmuir*, 2011, **27**, 109.
29 I. Martin-Fabiani, E. Rebollar, S. Perez, D. R. Rueda, M. C. Garcia-Gutierrez, A. Szymczyk, Z. Roslaniec, M. Castillejo and T. A. Ezquerra, *Langmuir*, 2012, **28**, 7938.
30 S. Y. Kim, A. Nunns, J. Gwyther, R. L. Davis, I. Manners, P. M. Chaikin and R. A. Register, *ACS Nano*, 2014, **14**, 5698–5705.
31 Y. Morikawa, T. Kondo, S. Nagano and T. Seki, *Chem. Mater.*, 2007, **19**, 1540.
32 Y. Zhang, J. L. Sargent, B. W. Boudouris and W. A. Phillip, *J. Appl. Polym. Sci.*, 2015, **132**, 41683.
33 J. Gong, A. Zhang, H. Bai, Q. Zhang, C. Du, L. Li, Y. Hong and J. Li, *Nanoscale*, 2013, **5**, 1195.
34 T. Pietsch, P. Müller-Buschbaum, B. Mahltig and A. Fahmi, *ACS Appl. Mater. Interfaces*, 2015, **7**, 12440.
35 T. Chen, D. P. Chang, R. Jordan and S. Zauscher, *Beilstein J. Nanotechnol.*, 2012, **3**, 397.
36 J. Zhang, Y. Li, X. Zhang and B. Yang, *Adv. Mater.*, 2010, **22**, 4249.
37 C. Lorch, H. Frank, R. Banerjee, A. Hinderhofer, A. Gerlach, G. Li Destri and F. Schreiber, *Appl. Phys. Lett.*, 2015, **107**, 201903.
38 T. Kassar, N. S. Güldal, M. Berlinghof, T. Ameri, A. Kratzer, B. C. Schroeder, G. Li Destri, A. Hirsch, M. Heeney, I. McCulloch, C. J. Brabec and T. Unruh, *Adv. Energy Mater.*, 2015, DOI: 10.1002/aenm.201502025.
39 N. Seidler, G. M. Lazzerini, G. Li Destri, G. Marletta and F. Cacialli, *J. Mater. Chem. C*, 2013, **1**, 7748.
40 K. Siow, S. Kumar and H. Griesser, *Plasma Processes Polym.*, 2015, **32**, 8.
41 C. W. Rochester, S. A. Mauger and A. J. Moule, *J. Phys. Chem. C*, 2012, **116**, 7287.
42 M. Schwartzkopf, A. Buffet, V. Körstgens, E. Metwalli, K. Schlage, G. Benecke, J. Perlich, M. Rawolle, A. Rothkirch, B. Heidmann, G. Herzog, P. Müller-Buschbaum, R. Röhlsberger, R. Gehrke, N. Stribeck and S. V. Roth, *Nanoscale*, 2013, **5**, 5053.
43 M. Schwartzkopf, G. Santoro, C. J. Brett, A. Rothkirch, O. Polonskyi, A. Hinz, E. Metwalli, Y. Yao, T. Strunskus, F. Faupel, P. Müller-Buschbaum and S. V. Roth, *ACS Appl. Mater. Interfaces*, 2015, **7**, 13547.
44 I. Martín-Fabiani, E. Rebollar, M. C. García-Gutiérrez, D. R. Rueda, M. Castillejo and T. A. Ezquerra, *ACS Appl. Mater. Interfaces*, 2015, **7**, 3162.
45 G. Li Destri, A. A. M. Gasperini and O. Konovalov, *Langmuir*, 2015, **31**, 8856.
46 G. Li Destri, T. Keller, M. Catellani, F. Punzo, K. D. Jandt and G. Marletta, *Macromol. Chem. Phys.*, 2011, **212**, 905.